Characterisation of polymeric network structures

Peters, R.

5 Low-molecular-weight model study of peroxide cross-linking of EP(D)M rubber using gas chromatography and mass spectrometry
Combination reactions of alkanes

Abstract

The combination reaction of linear and branched alkanes, initiated by dicumylperoxide, has been studied as a model for the combination cross-linking reaction of peroxide-cured terpolymerised ethylene, propylene and diene monomer. Both gas chromatography–mass spectrometry (GC–MS) and comprehensive two-dimensional GC–MS (GC×GC–MS) analyses have been employed to analyse the isomeric reaction products. The identification of these products based on their MS-fragmentation patterns is quite complex, due to the high tendency of random rearrangements. Careful elucidation of the high-mass ions at the optimised ionisation energy (55 eV) has resulted in proposed structures for the different isomeric reaction products. The structure assignment by MS is in agreement with the GC×GC elution pattern and with the result of a theoretical model to predict the boiling points and, thus, the GC retention times. In addition, a model that provided a direct correlation between chemical structure and retention times was developed, and this was found to provide a useful fit. Quantification of the identified reaction products by GC separation and flame ionisation detection allows classification according to the hydrogen abstraction sites for the alkanes by dicumylperoxide. The selectivity for hydrogen abstraction generally follows the expected order, but a higher reactivity was observed for the methylene group next to a primary methyl group, while a reduced reactivity of the methylene group next to ethyl and to methyl groups was observed.

R. Peters, D. Tonoli, M. van Duin, J. Mommers, Y. Mengerink, A.T.M. Wilbers, R. van Benthem, C.G. de Koster, P. Schoenmakers, Sj. van der Wal, Journal of Chromatography A, 1201 (2008)141-150.

5.1. Introduction

A copolymer of ethylene and propylene monomers (EPM) forms a chemically saturated, stable polymer backbone, which can be cross-linked with peroxides. A third non-conjugated diene monomer can be terpolymerised in a controlled manner to maintain a saturated backbone. The terpolymers are referred to as ethylene-propylene-diene rubber (EPDM). Cross-linked EP(D)M has excellent properties, especially its resistance to heat, ozone, and oxidation. This makes EP(D)M well suited for outdoor applications [1]. Different procedures can be used to cross-link EP(D)M. The most-applied one (>80%) is sulphur vulcanisation, which leads to C-S bonds and various types of S-S-bonds. Peroxide cross-linking, which yields more thermo-stable C-C bonds, and therefore excellent set properties over a wide temperature range [2], is the second most-common cross-linking technology. Both forms of cross-linking benefit from unsaturations, which are introduced by terpolymerisation of a small quantity (0–12%, *w/w*) of a diene monomer together with ethylene and propylene monomers. Dicyclopentadiene (DCPD) and 5-ethylidene-2-norbornene (ENB) are commercially used as dienes. The final properties of ethylene-propylene rubber (EPM) and ethylene-propylene-diene rubber (EPDM) depend to a large extent on the cross-link density, and on the chemical nature of the cross-links. Therefore it is important that the number as well as the nature of the cross-links can be determined. In general, two approaches can be distinguished to study cross-linked EP(D)M:

(1) *Direct analysis of the network*: The first and most applied approach is to analyse the cross-linked EP(D)M directly. This approach is preferred, but it suffers from several drawbacks, such as the large number of different cross-link structures formed at low concentration levels, the insolubility of the cross-linked EP(D)M, and the presence of additives (*e.g.* carbon black) in commercial EP(D)M products. This limits the applicable analytical techniques to mechanical analysis, spectroscopy and pyrolysis. Analysis of cross-linked EP(D)M with pyrolysis-gas-chromatography gives insight into the chemical composition of the EP(D)M [3]. Mechanical analysis gives insight in the properties of EP(D)M, such as tensile strength, elongation at break and compression set, which can be related to the network density [4]. Several spectroscopic techniques (FT-IR, Raman) yield information on the diene conversion [5], while solid-state nuclear-magnetic resonance (s-NMR) measurements provide information on the mobility of polymer

chain segments and have been used for quantification of the cross-link density [6–8]. The use of NMR spectroscopy for the characterization of cross-linked ^{13}C-labeled ENB-EPDM was shown by Winters *et al*. [9]. Recently, the kinetics of peroxide cross-linking of EPDM with different dienes (DCPD, ENB), in the absence of a co-agent, were studied using real-time FT-IR/Raman and real-time NMR relaxation-time measurements [10]. The different techniques described above have provided much valuable insight into EP(D)M networks, but they do not provide information on the chemical structure of the cross-links actually formed.

(2) *Indirect analysis of the network*: EP(D)M cross-linking can be studied indirectly by analysing "cross-linked" low-molecular-weight model compounds. The poor analytical accessibility of highly cross-linked systems makes the use of low-molecular-weight model compounds to mimic the cross-linking of polymers attractive. This has been shown by several cross-linking studies with model compounds, which led to elucidation of the mechanisms of accelerated sulphur vulcanisation of natural [11,12] and synthetic rubbers [13]. These studies resulted in an extended sulphur vulcanisation scheme. Van Drumpt and Oosterwijk [14] performed a study into peroxide cross-linking of polyethylene (PE) using model compounds. Although the study was performed on PE, the results give valuable insight into EP(D)M cross-linking. Camara *et al*. used electron spin resonance (ESR) spectroscopy to study cross-linking of (branched) alkanes [15] in terms of radical selectivity and rate constants for hydrogen abstraction. Low-molecular-weight model compounds were also used to study the effect of the type and amount of the third monomer on the peroxide-curing efficiency of EPDM [16].

These studies have shown that peroxide cross-linking of EPDM results from the combination of macro-radicals generated by the thermal decomposition of the peroxide and from the addition of macro-radicals to unsaturated moieties of other macromolecules [17] (*Fig.* 5.1). Although the presence of a diene monomer significantly enhances the peroxide-cross-linking efficiency, ethylene-propylene rubber (EPM), without a diene monomer, can be cross-linked by using peroxides through the combination of the macro-radicals (*Fig.* 5.1). The extent of the radical addition is determined by the number of residual unsaturations resulting from diene molecules and their structure (*e.g.* steric hindrance). The cross-linking efficiency is a linear function of the diene content [4].

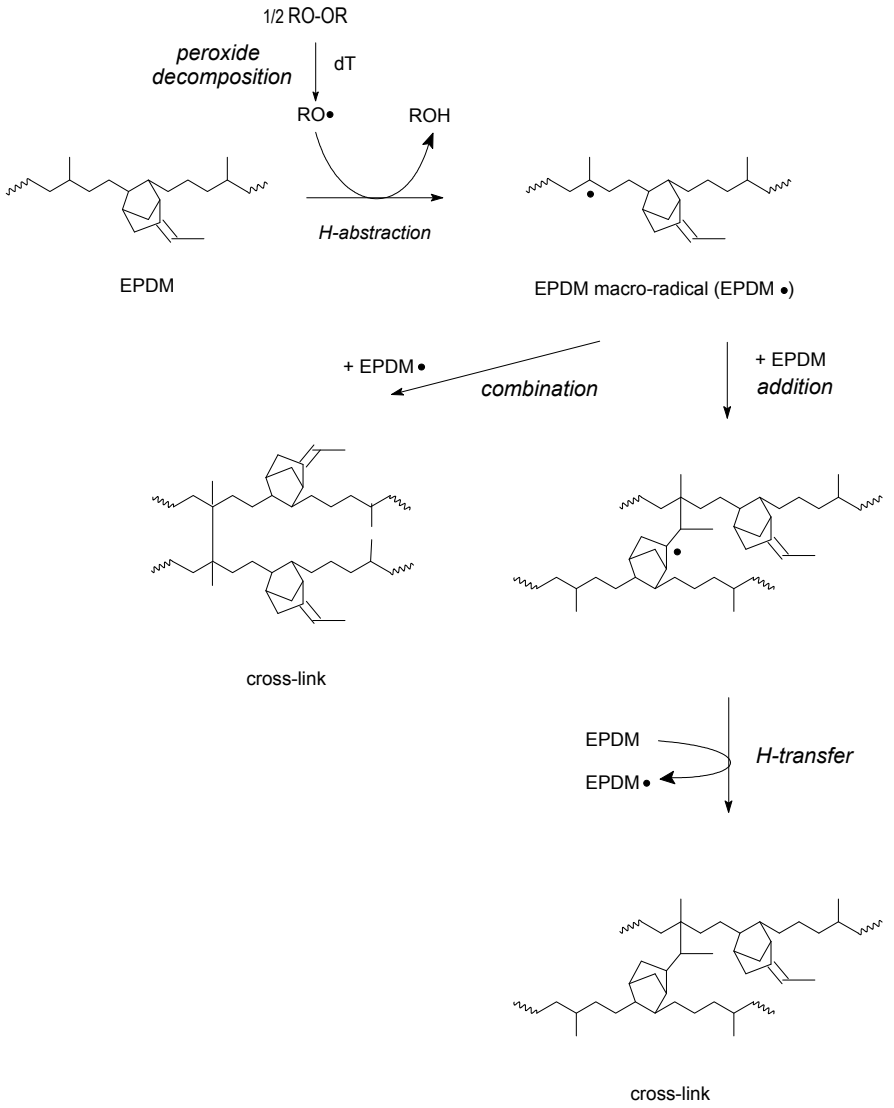

Fig. 5.1. General scheme for peroxide cross-linking of EPDM with ENB as a diene.

To enhance our understanding of the mechanism of EP(D)M peroxide cross-linking, which in turn can be used for obtaining more insight into the structure–property relationships, a more-detailed study of the chemistry of peroxide cross-linking is necessary. To mimic the combination reaction (*Fig.* 5.1), low-molecular-weight alkanes are "cross-linked", while the addition reaction is mimicked by "cross-linking" of alkanes and alkenes, under reaction conditions as close as possible to those of the actual peroxide cross-linking of EP(D)M.

Attack of the peroxide-derived radicals on the different positions in the alkanes/alkenes will result in a great variety of branched, isomeric reaction products. Analysis of these isomers will provide insight into the chemistry and the reactivity of the alkane- and alkene-radicals during the combination and addition reactions. To obtain this information, qualitative and quantitative analysis of the different reaction products is needed. Typically, this kind of information is achieved by chromatographic and mass-spectrometric techniques, such as gas chromatography–mass spectrometry (GC–MS) [18]. Unfortunately, the identification of the "high" molecular weight branched alkane isomers by MS is difficult, since they have a high tendency to undergo isomerisation before fragmentation upon electron ionisation at 70 eV. This results in very similar MS-spectra for the different branched isomeric alkanes [19]. To increase the reliability of the MS-identification, comprehensive two-dimensional GC–MS (GC×GC–MS) can be used. This technique is based on two consecutive GC-separations, typically according to boiling point and polarity. It allows group-type separations according to chemical classes, which results in ordered chromatograms [20]. Fortunately, the boiling points of branched alkanes depend strongly on the degree of branching and, consequently, the retention times of branched alkanes on a non-polar GC column show a good deal of variation [18]. To increase the reliability of the MS-identification of the different reaction products in our model study, the boiling point of these branched alkanes can be used to predict the retention time. For that purpose, the relation between retention time and boiling point [21] and the boiling point of the reaction products must be known. The lack of experimental boiling-point data of highly branched C11 alkanes and higher [22,23], makes the prediction of the elution order and the retention times for the branched reaction products difficult. To compensate for the lack of boiling-point data, the boiling points of branched alkanes up to C22 have been predicted by quantitative structure–property relationships (QSPRs) [24]. The QSPR model [24] describes the empirical relations between physical properties and graph-theoretical topological indexes. QSPRs are powerful tools to obtain simple models predicting the chromatographic behavior of different hydrocarbons [25–28]. The most accurate boiling points of alkanes with a low degree of branching, compared to other models [29], are obtained by a combination of the Hosoya index (*Z*, measure of the mode of branching) [30], the Wiener Path numbers (*P*, rough measure of the surface area) [30], and the methyl number (*Mth*, measure of the degree of branching) [29]. No direct model is available to predict the retention or boiling point of alkanes with a high degree of branching, which is probably due to the complex influence of steric effects on the boiling point.

In the present study of the peroxide cross-linking reaction we focus on the combination reactions between alkanes, while the study of addition reactions, which involves alkenes, will be described in a separate paper. The goal of this study is to explain the combination of alkanes, initiated by dicumylperoxide (DCP), in terms of structures and reactions, as a model for the combination reaction in peroxide-cured EP(D)M. *n*-Hexane, *n*-octane, *n*-decane, 2-methylpentane and 2-methylhexane have been employed as model compounds for EP(D)M. They were "cross-linked" with DCP to "higher" molecular weight alkanes. The combination reaction products of alkane with DCP were separated by GC, using a non-polar column, and by GC×GC, using a combination of a non-polar and a medium-polar column. Identification was performed by interpretation of the MS-fragmentation patterns. To increase the reliability of the elucidated structures, a QSPR model was used to predict the boiling point, and thus the retention time and the elution order. An even better prediction of the retention times may be obtained by a QSPR model correlating them directly with the chemical structure. The feasibility of these approaches for the studied compounds was demonstrated. The different reaction products were quantified and classified according to the H-abstraction sites for the alkanes. This provided valuable insight into the peroxide-initiated combination reactions.

5.2. Experimental

The reaction mixtures were prepared by dissolving 5% (*w/w*) dicumylperoxide (DCP, bis(α,-dimethylbenzyl)peroxide, >98%, Merck, Darmstadt, Germany) in *n*-hexane (>99%), *n*-octane (>99%), *n*-decane (>99%), 2-methylpentane (>99%) or 2-methylhexane (>99%), all purchased from Fluka (Buchs, Switzerland). A magnetic stirrer stirred these solutions in a nitrogen atmosphere at room temperature for two hours in a 3-mL pressure-resistant vial closed by a PTFE cap. The mixtures were subsequently stirred and heated for 30 min in an oil bath at 160°C. However, the mixtures that contained *n*-hexane or 2-methylpentane were heated at 135°C for 8 h to keep reasonable pressure in the vials. The reaction times have been designed in order to accomplish total decomposition of the peroxide at these temperatures (half-life time is 193 s at 160°C). The reaction products of the different alkanes with DCP are designated with numbers; the first two digits (**xx**_xx(Cx)xx(Cx)) represent the number of C-atoms in the longest chain (backbone). Each next two digits (xx_**xx**(Cx)**xx**(Cx)) show the position of a side chain on the backbone, while the length of each side chain is given between brackets (xx_xx(**Cx**)xx(**Cx**)). For example, 5,5,6,6-

tetramethyldecane is designated as 10_05(C1)05(C1)06(C1)06(C1).

The GC–MS experiments were performed on an Agilent 6890 GC and an Agilent 5973 MSD system (Agilent, Avondale, PA, USA). The capillary column used was a CP-Sil 5 CB low-bleed MS (100% dimethylpolysiloxane phase, 325°C maximum, 30.0m×0.25mm, d_f 0.25_m) (Varian, Palo Alto, CA, USA). The GC oven was programmed from 40°C (1min isothermal) to 280°C, at a rate of 1°C/min. Helium was used as the carrier gas with a constant flow (1 mL/min). The samples were injected undiluted (1 μL) using a split injection (split ratio 25:1) at 250°C. The GC experiments to relate boiling point with retention time were performed on the same GC system, using a mixture of approximately 1% (*w/w*) of *n*-alkanes from C7 up to C22 and isoalkanes up to C9, which were diluted in *n*-hexane (>99%, all purchased from Sigma–Aldrich, St. Louis, MO, USA). The quantification experiments were performed using GC-flame-ionisation detection (FID). The same GC conditions were used as described before. The FID signal was collected with Atlas 2002, version 6.18, data-management system (Thermo Labsystems, Manchester, UK).

The GC×GC–MS was performed on an Agilent 6890N GC system and a Leco Pegasus III time-of-flight MS (Leco, St. Joseph, MI, USA) system. A non-polar capillary column VF-1MS (100% dimethylpolysiloxane phase, 50m×0.25mm, d_f 0.4 μm; Varian) was used for the first separation dimension and a medium-polar capillary column VF-17MS (50% phenyl and 50% dimethylpolysiloxane phase, 1.5m×0.1mm, d_f 0.2 μm; Varian) for the second dimension. The columns were coupled using a universal press-fit (Varian). The constant helium flow was 1.2 mL/min. The samples were injected (1 μL) using a split injection (split ratio 1:100) at 280°C. The GC oven was programmed from 40°C (3 min isothermal) to 300°C (10 min isothermal) at 2°C/min. The temperature of the second-dimension column was maintained 5°C above the temperature of the first-dimension column during the entire analysis. The modulator offset was 20°C. The MS-spectrum was scanned from *m/z* 20 to 550, with a scan rate of 150 spectra/s. The ion source was set at 250°C and the ionisation energy was 70 eV.

To confirm the MS-identification, the main reaction product of 2-methylhexane was fractionated with preparative GC and the fractions were subjected to NMR analysis. The GC separation was performed on an Agilent 6890 GC system. The capillary column used was a CP-Sil 5 CB (50.0m×0.53mm, d_f 5 um; Varian). The GC oven was programmed from 50 to 150°C, at 10°C/min, to 280°C, with 5°C/min. The injection volume was 3 μL (splitless, 250°C) and 77 fractions of the main reaction product of 2-methylhexane (t_R = 26 min) were collected using a preparative fraction collector (Gerstel, Mülheim an der Ruhr, Germany). The ^{1}H-NMR measurements were performed using a Varian Inova 600MHz NMR

Spectrometer. The fractionated compound was dissolved in $CDCl_3$, while the spectrum was recorded using 32 scans and 3 s relaxation time. Three different two-dimensional (2D) NMR techniques were also applied; gCOSY (8 scans per increment, 256 increments, relaxation delay 1.3 s, ^{1}H sweep width 4801.9 Hz, processing with sine bell function, measurement time 53 min), gHSQC (4 scans per increment, 2×128 increments, relaxation delay 1.3 s, processing with Gaussian function, measurement time 27 min) and gHMBC (32 scans, 400 increments, relaxation delay 1 s, processing with sine bell function, measurement time 4 h 20 min). ACD software (ACD/CNMR Predictor, ACD/Labs, Toronto, Canada) was used to verify the identification by NMR.
The calculation of the Hosoya index (Z), the Wiener Path numbers (^1P, ^2P, . . ., ^6P) and the methyl number (Mth) has been described by Burch *et al*. [29]. The equation used to estimate the boiling point (bp) is obtained from Burch *et al.* [29];

$$bp(^1P,\ ^2P,\ .\ .\ .\ ,\ ^6P,\ Mth,\ Z) = 847.41474 + 221.61698(^1P)^{0.49420} - 1182.20853(^2P)^{0.03689} + 0.00125(^3P)^{3.39724} - 3.02445(^4P)^{0.93751} - 2.16070(^5P)^{1.01631} - 0.56366(^6P)^{1.38233} - 2.10575Mth^{0.5695} - 9.61075Z^{0.19907} \quad (1)$$

The relation between structure parameters and experimental retention times was investigated using Matlab with the PLS toolbox (R2007a, The MathWorks, Natick, MS, USA). The statistics toolbox was also used as an Excel Add-in XLStat (Addinsoft SARL, Andernach, Germany).

5.3. Results

5.3.1. Qualitative analysis of alkane/peroxide reaction products

In order to study the combination reactions, the various reaction mixtures of the different alkanes with DCP were analysed by GC–MS and GC×GC–MS before and after the "cross-linking" reaction. A typical GC–MS chromatogram of the reaction products of *n*-octane with DCP is shown in *Fig.* 5.2. The GC×GC–MS chromatogram of the same reaction mixture is depicted in *Fig.* 5.3.

5.3.1.1. Identification of DCP decomposition products

In all reaction mixtures the concentration of DCP after the reaction was less than

0.1% (*w/w*). Two main peroxide decomposition products were identified: 2-phenylpropan-2-ol and acetophenone (*Fig.* 5.2). Small concentrations of these DCP decomposition products were also observed before reaction, as a consequence of some premature decomposition of DCP during storage or of the high injection temperature (250°C). 2-Phenylpropane-2-ol is formed via hydrogen abstraction from the alkane substrates by the cumyloxy-radical, while acetophenone is formed via beta-scission of the cumyloxy-radical, yielding a methyl-radical as secondary radical. No indication was found for the dehydratation of 2-phenylpropan-2-ol into α-methylstyrene. Coupling products of cumyloxy- and alkane-radicals were not observed. This indicates that the cross-linking proceeds via hydrogen abstraction from the alkane by the peroxide-radicals.

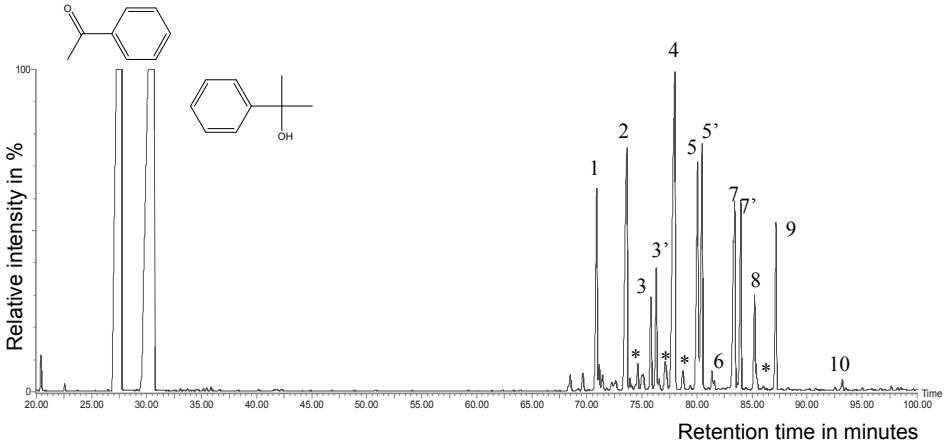

Fig. 5.2. GC–MS chromatogram of the reaction products of n-octane with 5% (w/w) DCP. The peaks designated with numbers refer to octane dimers as explained in Table 5.1, while the peaks designated with '' are unsaturated octane dimers. For conditions, see Section 5.2.*

5.3.1.2. Identification of alkane reaction products by GC–MS and GC×GC–MS

The identification of the various alkane reaction products by GC–MS is illustrated hereafter, using the reaction products of *n*-octane and DCP as an example (see also *Figs.* 5.2 and 5.3). Based on GC×GC–MS analysis, three different groups can be distinguished in the class of the various alkane reaction products. The first (peaks 1–5 and 7) and second group (peaks 6, 8 and 9) are identified, based on the molecular ion (*m/z* $M^{\bullet+}$ = 226), as isomeric, saturated

alkanes with formula $C_{16}H_{34}$. These octane dimers are formed via the combination of two octyl-radicals. Since hydrogen abstraction can take place from each C-atom, and since each corresponding octyl-radical can participate in combination reactions, a complex mixture of isomeric $C_{16}H_{34}$ species is the result. No octane trimers are observed. The third group observed in the GC×GC–MS chromatogram (assigned by '*') is identified as isomeric, unsaturated hydrocarbons with formula $C_{16}H_{32}$ (m/z $M^{\bullet+}$ = 224). The MS-spectra of these compounds are dominated by a series of $C_nH_{2n-1}^{+}$ ion peaks and peaks originating from the loss of a $C_nH_{2n+1}^{\bullet}$ radical from the molecular ion, which indicate the presence of a double bond in these octane dimers. Besides these unsaturated octane dimers, traces of *n*-octene isomers were observed.

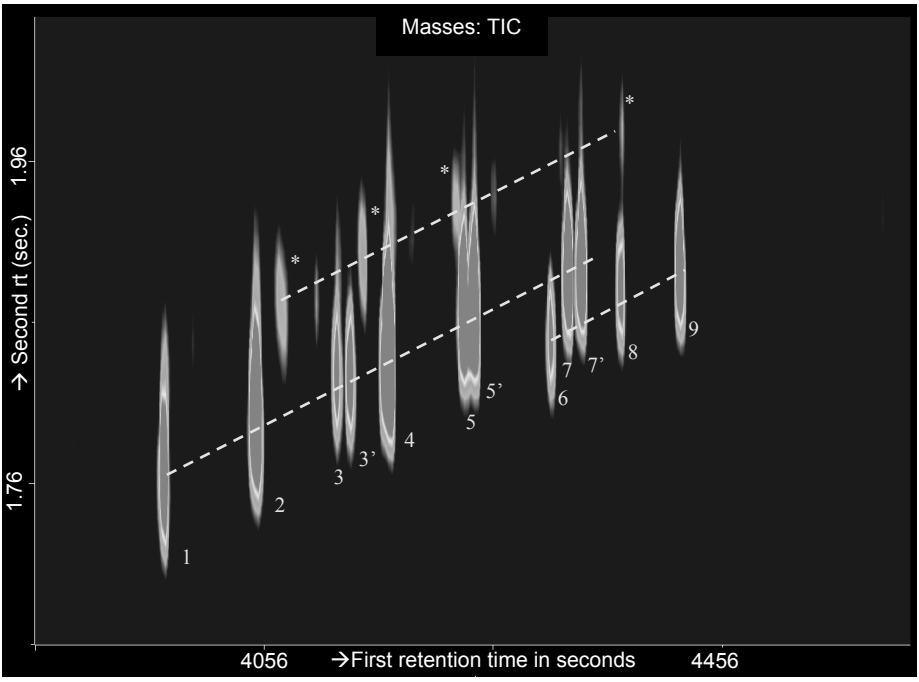

Fig. 5.3. GC×GC–MS chromatogram of the reaction products of n-octane with 5% (w/w) DCP. The peaks designated with numbers refer to octane dimers as explained in Table 5.1, while the peaks designated with '' are unsaturated octane dimers. See Section 5.2 for GC×GC–MS conditions.*

In order to learn more about the formation and the reactivity of octyl-radicals during the combination reaction, the structure of the saturated isomeric octane dimers ($C_{16}H_{34}$) was elucidated using EI-fragmentation of their molecular ion. The EI-MS spectra of these octane dimers are dominated by an abundance

maximum around ion peaks at *m*/*z* 43 ($C_3H_7^+$), *m*/*z* 57 ($C_4H_9^+$) and *m*/*z* 71 ($C_5H_{11}^+$). The highly intense radical cation peak at *m*/*z* 112 ($C_8H_{16}^{\bullet+}$) is formed by δ-cleavage and hydrogen shift of the octyl chain at the branching point of the octane dimer, which is characteristic for these branched octane dimers. At low abundance (<1%) characteristic *m*/*z* peaks indicative of chain branching are observed. These *m*/*z* peaks are formed by δ-cleavage ($C_nH_{2n+1}^+$) and, to a lesser extent, by charge retention ($C_nH_{2n}^{\bullet+}$) at the branching C-atom. These high-mass ions are indicators of the location of the branching point and, therefore, important for elucidating the branched structure. To increase the intensity of these high-mass ions, the electron-ionisation energy was decreased systematically (70, 60, 50, 40, and 30 eV). The peak intensity of some characteristic ions at different ionisation energies is shown in *Fig.* 5.4. The high-mass ions peak intensities are still low, but tend to a maximum at 55 eV (approximately 2–5% of the base peak).

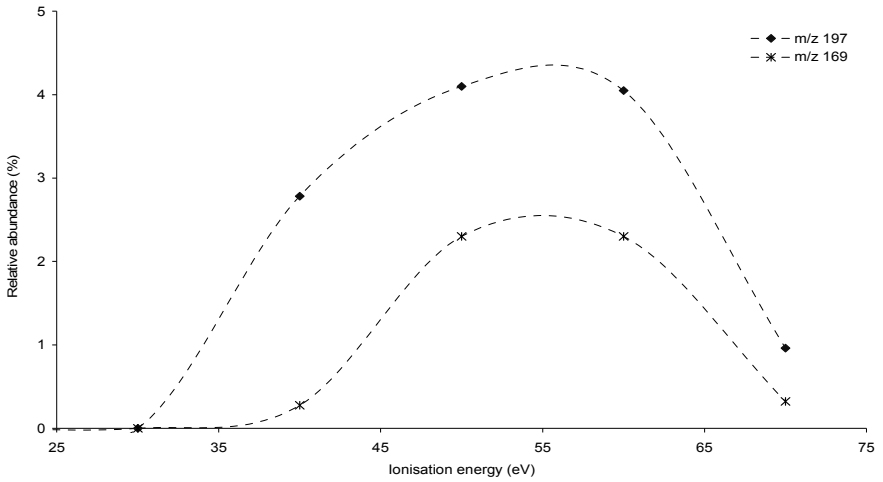

Fig. 5.4. Relative EI-MS-intensity vs. electron-ionisation energy of the reaction product of n-octane with DCP at t_R 73.62 min.

The branching point of the octane dimers is elucidated by studying the loss of $C_nH_{2n+1}^{\bullet}$ radical by the primary δ-cleavage fragmentation reaction at 55 eV. A typical MS-spectrum at 55 eV is shown in *Fig.* 5.5, with characteristic ions that are observed at *m*/*z* 183, *m*/*z* 169 and *m*/*z* 141. In the case of *n*-octane, *m*/*z* 183 and *m*/*z* 169 are indicative of branching at the fourth position of the octyl chain, while *m*/*z* 141 is indicative of branching at the second position of the octyl chain. This compound is thus identified as 5-propyl-6-methyldodecane (12_05(C3)06(C1)).

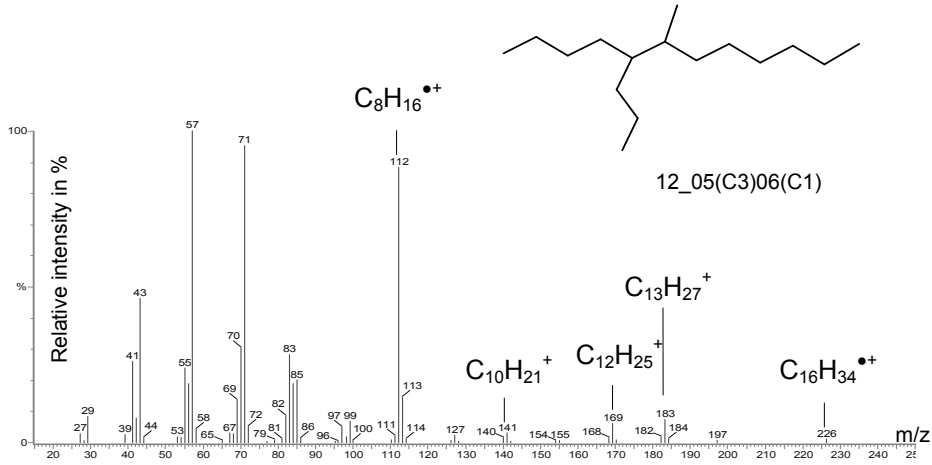

Fig. 5.5. Typical EI-MS-spectrum (55 eV) of one of the octane dimer reaction products at t_R 77.97 min.

The observed characteristic ions for different compounds of the various octane dimers are collected in Table 5.1. The *m*/*z* 127 ion is often observed. Formation of this fragment ion is due to the loss of $C_7H_{15}^{\bullet}$. This is probably the result of a secondary fragmentation. Secondly, in some cases the MS-interpretation fits to more than one structure. This is caused by the absence of $CH_3^{\bullet}$ cleavage, since the loss of the largest alkyl group is more favourable. The low abundance of *m*/*z* peaks originating from these ions and the absence of methyl-cleavage information make these indicators of the branching structure less reliable. Since each octyl-radical can participate in combination reactions, 10 saturated isomeric octane dimers ($C_{16}H_{34}$) can theoretically be formed. GC–MS analysis shows more than 10 isomeric octane dimers in the reaction mixture of *n*-octane and DCP. Secondly, the observed fragmentation (Table 5.1) is identical for some of the reaction products of *n*-octane (*e.g.* t_R = 80.03 and 80.45 min), which indicates that these reaction products have the same branching point. This can be explained by the fact that these octane dimers have two chiral centres (except 13_05(C3), 14_06(C2) and 15_07(C1), which have only one chiral centre). This gives rise to the occurrence of diasteromers or mesomers in the case of 10_05(C3)06(C3), 12_06(C2)07(C2), and 14_07(C1)08(C1). The different diasteromers and mesomers can have different physical properties, which makes it possible to separate them on a non-chiral GC-column. Sometimes, the differences in physical properties are so small that just one peak is observed. Separation of the diasteromers/mesomers is beyond the scope of the research reported here.

Table 5.1. Structure proposals for saturated dimer reaction products of n-alkanes with DCP based on EI-MS spectra and t_R calculated with different QSPR models

Sub.	Peak №	$t_{R\ (exp)}$ (min)	Characteristic ions (loss of $C_nH_{2n+1}^{\bullet}$)	Identified structure (*)	$t_{R\ (indirect\ QSPR)}$ (min)	$t_{R\ (direct-QSPR)}$ (min)
n-Octane						
	1	70.86	127, 169, 183	10_05(C3)06(C3)	59.22	70.49
	2	73.62	127, 155, 169, 183, 197	11_05(C3)06(C2)	70.25	74.06
	3	75.80	127, 155, 197	12_06(C2)07(C2)	76.60	76.38
	3’	76.28	127, 155, 197	12_06(C2)07(C2)	76.60	76.38
	4	77.97	127, 141, 169, 183	12_05(C3)06(C1)	75.23	76.81
	5	80.03	127, 141, 155, 197	13_06(C2)07(C1)	80.28	80.06
	5’	80.45	127, 141, 155, 197	13_06(C2)07(C1)	80.28	80.06
	6	83.28	127, 169, 183	13_05(C3)	83.06	82.26
	7	83.41	141	14_07(C1)08(C1)	83.39	83.73
	7’	83.95	141	14_07(C1)08(C1)	83.39	83.73
	8	85.22	127, 155, 197	14_06(C2)	86.21	85.36
	9	87.17	141	15_07(C1)	87.54	88.10
	10	93.18	127, 141, 155, 169, 183, 197	16	93.42	94.28
n-Hexane						
	11	30.35	99, 127, 141	08_04(C2)05(C2)	29.23	29.41
	11’	30.53	99, 127, 141	08_04(C2)05(C2)	29.23	29.41
	12	32.86	99, 113, 127, 141	09_04(C2)05(C1)	32.06	33.28
	12’	33.08	99, 113, 127, 141	09_04(C2)05(C1)	32.06	33.28
	13	34.96	99, 113, 155	10_05(C1)06(C1)	33.66	34,70
	13’	35.45	99, 113, 155	10_05(C1)06(C1)	33.66	34.70
	14	37.32	99, 127, 141	10_04(C2)	36.46	37.75
	15	38.24	99, 113, 155	11_05(C1)	37.68	39.02
	16	44.09	99, 113, 127, 141, 155	12	44.35	44.04
n-Decane						
	17	107.71	155, 211, 225	12_06(C4)07(C4)	101.66	107.74
	18	111.66	155, 197, 211, 225, 239	13_06(C4)07(C3)	106.60	111.18
	19	116.41	155, 197, 239	14_07(C3)08(C3)	111.13	116.66
	19’	116.52	155, 197, 239	14_07(C3)08(C3)	111.13	116,66
	20	119.32	155, 183, 211, 225, 253	14_05(C4)06(C2)	114.30	119.87
	21	121.68	155, 183, 197, 239, 253	15_06(C3)07(C2)	118.71	121.95
	21’	121.89	155, 183, 197, 239, 253	15_06(C3)07(C2)	118.71	121.95
	22	124.10	155, 211, 225, 253 (low)	14_06(C4)07(C2)	119.32	123.69
	23	125.89	155, 197, 239	16_07(C3)08(C1)	123.65	125.60
	23’	125.98	155, 197, 239	16_07(C3)08(C1)	123.65	125.60
	24	126.09	155, 183, 253	16_08(C2)09(C2)	126.26	126.20
	24’	126.26	155, 183, 253	16_08(C2)09(C2)	126.26	126.20
	25	127.60	155, 211, 225	16_06(C4)	122.34	127.04
	26	128.15	155, 197, 239	17_07(C3)	125.08	128.55
	27	128.63	155, 183, 253	17_08(C2)09(C1)	129.70	128.32
	27’	128.75	155, 183, 253	17_08(C2)09(C1)	129.70	128.32
	28	129.54	155, 169, 183	18_09(C1)10(C1)	132.11	130.05

	28’	129.58	155, 169, 183	18_09(C1)10(C1)	132.11	130.05
	29	129.59	155, 183, 253	18_08(C2)	129.64	130.71
	30	129.91	155, 169, 267 (w)	19_09(C1)	131.35	129.26

** the first two digits (xx_xx(Cx)xx(Cx)) indicate the length of the backbone, each next two digits (xx_xx(Cx)xx(Cx) show the position of the side chain on the backbone, while the length of the side chain is given between brackets (xx_xx(Cx)xx(Cx)).*

Table 5.2. Structure proposals of reaction products of isoalkanes with DCP based on EI-MS spectra and t_R calculated with different QSPR models

Sub.	Peak №	$t_{R\ (exp)}$ (min)	Characteristic ions (loss of $C_nH_{2n+1}^{\bullet}$)	Identified structure (*)	$t_{R\ (indirect\ QSPR)}$ (min)	$t_{R\ (direct-QSPR)}$ (min)
2-Methylpentane						
	31	23.96	99, 113 (high), 127	08_02(C1)04(C1) 05(C1)07(C1)	24.79	25.24
	31’	24.11	99, 113 (high), 127	08_02(C1)04(C1) 05(C1)07(C1)	24.79	25.24
	32	26.06	99, 113, 127 (high)	07_02(C1)04(C1) 05(C2)06(C1)	27.10	28.09
	32’	26.45	99, 113, 127 (high)	07_02(C1)04(C1) 05(C2)06(C1)	27.10	28.09
	33	26.85	99, 113, 127	08_02(C1)04(C1) 05(C1)05(C1)	28.63	27.10
	34	27.49	99, 127 (high), 155	06_03(C3)04(C3)	28.19	29.23
	34’	27.64	99, 127 (high), 155	06_03(C3)04(C3)	28.19	29.23
	35	29.67	99, 113, 127	07_02(C1)03(C2) 04(C1)04(C1)	30.67	29.85
	36	34.13	113	09_02(C1)04(C1) 06(C1)	32.28	34.75
	37	35.11	85 (high) 99, 127	08_04(C1)04(C1) 05(C1)05(C1)	36.53	34.02
	38	37.16	127	09_04(C1)04(C1) 06(C1)	34.99	32.37
2-Methylhexane						
	39	40.50	99, 113, 141, 169	08_02(C1)04(C2) 05(C2)07(C1)	41.69	40.93
	39’	41.07	99, 113, 141, 169	08_02(C1)04(C2) 05(C2)07(C1)	41.69	40.93
	40	43.26	99, 113, 155 (high)	08_02(C1)04(C2) 05(C3)	42.04	42.61
	40’	44.40	99, 113, 155 (high)	08_02(C1)04(C2) 05(C3)	42.04	42.61
	41	44.94	99, 113, 127, 141, 169	08_04(C3)05(C3)	43.44	45.49
	41’	45.23	99, 113, 127, 141, 169	08_04(C3)05(C3)	43.44	45.49
	42	47.18	99, 113, 127, 141, 155, 169	10_02(C1)04(C2) 06(C1)	48.86	50.97
	43	48.04	99, 113, 127, 141, 155	09_02(C1)04(C2) 05(C1)08(C1)	48.65	49.55

44	48.71	99, 113, 127	09_04(C3)05(C1) 08(C1)	50.29	49.05
45	50.09	99, 113, 141, 155, 169	10_02(C1)05(C1) 06(C1)09(C1)	51.93	50.08
46	50.38	99, 141, 155, 169	09_02(C1)04(C2) 05(C1)05(C1)	48.10	51.89
47	50.96	99, 113, 127, 141 (high)	10_02(C1)05(C1) 06(C1)06(C1)	51.99	51.50
48	51.32	99, 113, 127, 141, 155, 169	09_04(C3)05(C1) 05(C1)	50.10	50.91
49	51.69	99, 113, 127, 141, 155, 169	10_04(C3)06(C1)	50.15	51.80
50	53.34	99, 141, 151 (low)	11_05(C1)05(C1) 07(C1)	49.93	51.20
51	54.81	99, 113, 127, 141, 155, 169	11_02(C1)05(C1) 07(C1)	54.25	53.27
52	58.52	99, 141 (s), 155, 169	10_05(C1)05(C1) 06(C1)06(C1)	59.25	58.06
53	59.00	99, 113, 141, 169	12_05(C1)08(C1)	57.78	56.46

* *the first two digits (xx_xx(Cx)xx(Cx)) indicate the length of the backbone, each next two digits (xx_xx(Cx)xx(Cx) show the position of the side chain on the backbone, while the length of the side chain is given between brackets (xx_xx(Cx)xx(Cx)).*

The GC–MS study of the reaction products of *n*-hexane and *n*-decane with DCP gives similar GC–MS results to those observed for *n*-octane. The elucidation of the MS-spectra of the reaction products of *n*-decane with DCP has resulted in the structure proposals as outlined in Table 5.1. The GC–MS analysis of the reaction products of 2-methylpentane with DCP revealed several reaction products, which could be identified as isomeric, saturated alkanes with formula $C_{12}H_{26}$ (m/z $M^{\bullet+}$ = 170). All reaction products show a highly intense peak at m/z 85, resulting from δ-cleavage of the C6-chain at the branching point, which is characteristic for these 2-methylpentane dimers. The MS-spectra of all the compounds are very similar. The characteristic ions, which are indicative for the different branching points, are listed in Table 5.2. The same observations are made for 2-methylhexane, as shown in Table 5.2.

5.3.1.3. Identification of alkane reaction products by QSPR

As discussed above, the identification of the branched alkane dimers using GC–MS is quite complex, since the MS-spectra are very similar for the different branched alkanes. This is especially true for the reaction products of the isoalkanes. In general, NMR can be used for identification of the branched products. However, the reaction mixtures contain many different reaction products, which results in impractically complex NMR spectra. In order to use

NMR as an identification tool, the reaction products must be isolated. Fractionation with preparative GC was performed for the main product of 2-mehylhexane and the resulting fraction was analysed by ^{1}H-NMR. The main reaction product (t_R = 58.52 min) of 2-methylhexane with DCP was identified as 5,5,6,6-tetramethyldecane (10_05(C1)05(C1)06(C1)06(C1)). Principally, this procedure is the best approach to identify the reaction products, but it is much too laborious for the identification of all the products in the different reaction mixtures.

Another possible approach to verify the MS-identification is to predict the retention behaviour of the branched alkanes. In general, the retention time of branched alkanes on a GC column of non-polar nature correlates strongly with the boiling point of the branched alkanes. The boiling point increases with increasing molecular weight, while it decreases with increasing degree of branching due to steric effects of the neighbouring groups of secondary, tertiary and quaternary C-atoms [18]. To predict the retention, a QSPR model [24] was used to estimate the boiling points. This data was used to predict the retention and elution order using a GC separation with known retention time/boiling point relation. The applicability of the QSPR model was tested using *n*-alkanes and isoalkanes with known boiling points.

First, the boiling points of *n*-alkanes (C7 up to C22) and isoalkanes up to C9 with known boiling points [22,23] were calculated with the QSPR model [29], using a combination of Wiener Path numbers, methyl indices, and Hosoya indices. The deviation between the calculated and experimental boiling points from the literature is <1.0% for all the different alkanes used. However, an increasing systematic deviation in predicted boiling point is observed for the higher *n*-alkanes (C18 and higher). This is directly related to the used model [24], which is mainly based on low-molecular-weight branched alkanes.

Next, the relation between the retention times (t_R) and the calculated boiling points of *n*-alkanes (C7 up to C22) and isoalkanes up to C9 was established using a non-polar GC column. The relation between the retention time and the calculated boiling point is non-linear, especially for the smaller linear and branched alkanes;

$$t_R\ (\text{min}) = 1.15 \times 10^{-7}(\text{bp(QSPR)})^4 - 1.26 \times 10^{-4}(\text{bp(QSPR)})^3 + 5.06 \times 10^{-2}(\text{bp(QSPR)})^2 - 8.17(\text{bp(QSPR)}) + 468.27 \quad (2)$$

Finally, the QSPR model was used to calculate the boiling points of the branched octane dimers of the DCP “cross-linking” reaction mixture of *n*-octane, which were then converted into retention times. The results (Table 5.1)

show that the boiling point, and thus the retention time, decreases with increasing branching. The calculated elution order fits very well to the compounds identified by MS. The only exceptions are the elution order of 12_06(C2)07(C2) and 12_05(C3)06(C1), which are reversed. This is probably due to the fact that the calculated boiling point of these compounds is almost the same, the difference being less than 2°C. In general, the deviation between calculated and experimental retention times is less than 1 min, except for the highly branched octane dimers, which show a systematic deviation up to 12 min (see also Table 5.1).

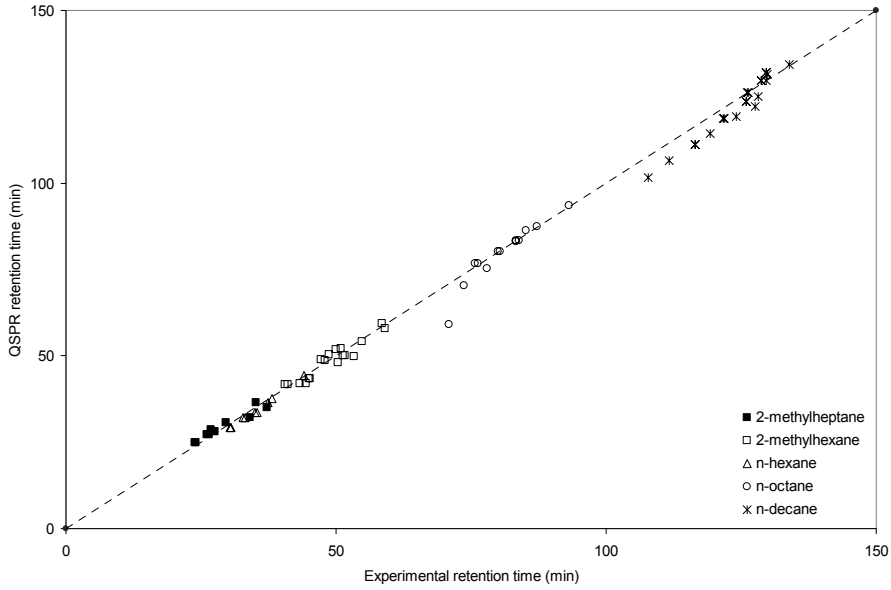

Fig. 5.6. Correlation of QSPR calculated via boiling point and experimental retention times of the reaction products of n-alkanes/isoalkanes with DCP (line is guide to the eye).

Similar results were found for the DCP "cross-linked" reaction products of *n*-hexane, *n*-decane, 2-methylpentane and 2-methylhexane, as outlined in Tables 5.1 and 5.2. The calculated retention times are plotted versus the experimental retention times in *Fig.* 5.6. The deviations are seen to be small (<1 min), except for the long-chain branched hydrocarbons (*e.g.* propyl and butyl side-chains). The highly branched reaction products of the methylalkanes show deviations between the calculated the experimental retention times up to 2 min, which are systematically higher than observed for the reaction products of *n*-alkanes. Both deviations originate from the increasing steric influence on the retention with increasing length and number of side chains. This effect is not included in the

QSPR model, since the model was constructed for the prediction of the boiling points of low-molecular-weight branched alkanes. The steric influence is also not included in the empirical relation between retention time and boiling point. This makes the prediction of the retention times for the long-chain (butyl, propyl) and highly branched reaction products less accurate.

The relationship used from structure parameters via boiling points to retention times is an indirect QSPR model. A systematic deviation for long-chain and highly branched reaction products was observed using this indirect relation. To address this problem, a direct relationship between the experimental GC–MS retention times and the structure parameters of the different branched alkanes (direct QSPR model) was investigated. The correlation with the highest predictive power was determined using the Wiener Path number from 1*P* up to 8*P*, combined with the *Z* and *Mth* values. The correlation of predicted retention times (t_R) using the structural parameters is;

$$t_R({}^1P, {}^2P, \ldots, {}^8P, Mth, Z) = -64.52704 + (X_0{}^1P + X_1{}^2P + \cdots + X_7{}^8P + X_8 Mth + X_9 Z) + (X_{10}{}^1P^2 + X_{11}{}^2P^2 + \cdots + X_{18} Mth^2 + X_{19} Z^2) + (X_{20}{}^1P^3 + X_{21}{}^2P^3 + \cdots + X_{28} Mth^3 + X_{29} Z^3) + (X_{30}{}^1P^4 + X_{31}{}^2P^4 + \cdots + X_{38} Mth^4 + X_{39} Z^4) \quad (3)$$

The model parameters ($X_0 \ldots X_{39}$) are given in Table 5.3, while the goodness-of-fit statistics is given in Table 5.4. A squared correlation coefficient (R^2) of 0.999 and a standard deviation using the "leave-one-out" principle (*RMSE*) of 1.7 min shows that the correlation has a good predictability of the data. Extending the validation set to 10 experiments causes an increase of the *RMSE* to 1.9 min. The deviation of the retention times from the direct-QSPR model and from the indirect QSPR model are plotted versus the experimental retention time in *Fig.* 5.7. The *SD* of the direct QSPR model (1.31 min) is significantly better than that of the indirect QSPR model (2.43 min; see Table 5.5). This is due to the increased systematic deviation of the calculated retention times for long-chain branched reaction products (*SD* 2.75 min) using the indirect model. For the direct-QSPR model the calculated retention times of the long-chain branched hydrocarbons (C12, C16 and C20) are in very good agreement with the experimental retention times (*SD* 0.57 min). The deviation of the methylalkane reaction products is not improved using the direct QSPR correlation instead of the indirect QSPR relation. These compounds show an even higher deviation (*SD* 1.66 min) than the long-chain branched alkanes. This is probably caused by the fact that the structural parameters used are not sufficiently descriptive to discriminate unequivocally between the different highly branched methylalkane reaction products (C12, C14).

Table 5.3. Direct QSPR model parameters

	a = 0	a = 1	a = 2	a = 3
X_{a0}	9.92832	3.35437×10^{-1}	0	0
X_{a1}	-2.67845	1.95942×10^{-1}	-5.81670×10^{-3}	0
X_{a2}	$-1.93618\times10^{+1}$	1.10817	-1.90755×10^{-2}	0
X_{a3}	6.74932	-4.52594×10^{-1}	7.71326×10^{-3}	0
X_{a4}	$1.63415\times10^{+1}$	-2.18787	1.10298×10^{-1}	-1.94739×10^{-3}
X_{a5}	7.52257×10^{-1}	-3.74615×10^{-1}	2.43451×10^{-2}	-4.80806×10^{-4}
X_{a6}	-9.65003×10^{-2}	-1.97995×10^{-1}	9.69867×10^{-3}	0
X_{a7}	4.49565	-1.14139	1.00642×10^{-1}	-2.79369×10^{-3}
X_{a8}	-1.44770	8.77157×10^{-1}	-1.91423×10^{-1}	0
X_{a9}	2.04821×10^{-2}	-1.06571×10^{-5}	1.15243×10^{-9}	0

Table 5.4. Goodness-of-fit statistics direct QSPR model

Goodness-of-fit	
Observations	72
DF	30.0
R_2	0.999
SSE	89.532
MSE	2.984
RMSE	1.728

Table 5.5. Standard deviation (SD) of difference between experimental and calculated retention time by both the direct and indirect QSPR model

Class of compounds	*SD* indirect QSPR	*SD* direct QSPR
All reaction products	2.43	1.31
Methyl alkanes	1.52	1.66
Alkanes without **C3/C4** side chains	1.08	0.59
Alkanes with **C3/C4** side chains	2.75	0.57

The use of GC×GC elution patterns and direct and indirect QSPR models to predict retention times greatly increases the reliability of the identification of branched alkanes by MS. The observed GC×GC elution pattern and the predicted GC–MS elution order of the reaction products are in very good agreement with the MS-identification.

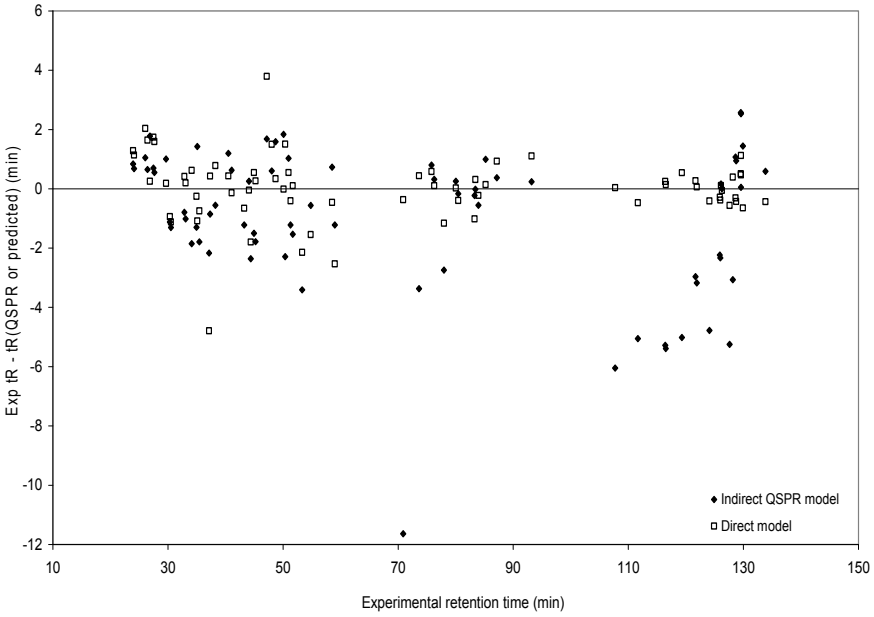

Fig. 5.7. Deviation of the calculated retention time using the direct and indirect QSPR models (min) vs. the experimental retention time.

5.3.2. Quantitative analysis of alkane reaction products by GC-FID

The different DCP "cross-linked" reaction products of *n*-alkanes and isoalkanes are quantified (in triplicate measurements) using GC-FID with *n*-dodecane as an internal standard. The used GC-conditions are similar to the conditions used for the GC–MS experiments. The GC-FID measurements yielded relative concentrations of the different isomers formed versus the branching position. This allowed calculation of the radical selectivity, which is given in Tables 5.6 and 5.7. The cross-linking process starts with the thermal decomposition of the peroxide as it initiates the free-radical reaction, followed by hydrogen abstraction of the alkanes. The selectivity of hydrogen abstraction from the C-H bonds of the alkanes follows the expected order [31,32], *i.e.* tertiary > secondary > primary CH. The low concentration of primary radicals is in agreement with the lower susceptibility for hydrogen abstraction of the primary methyl group. Hydrogen abstraction from methylene groups of the *n*-alkanes occurs to a higher extent and roughly follows the statistical distribution of the various methylene groups (CH_3-$\boldsymbol{CH_2}$-CH_2-R and R-CH_2-$\boldsymbol{CH_2}$-CH_2-R). When inspecting the data in more detail, we find the probability for hydrogen abstraction from the methylene

group next to a primary methyl group (CH_3-***CH_2***-CH_2-R) to be higher than expected from just the statistical distribution. In contrast, hydrogen abstraction from the methylene group next to an ethyl group (CH_3-CH_2-***CH_2***-CH_2-R) turns out to occur systematically less frequently. A similar lack of reactivity is observed for the isoalkanes, which show a decreasing tendency for hydrogen abstraction from the methylene group next to an ethyl group and the methylene group next to a tertiary methine group (($CH_3)_2$-CH-***CH_2***-CH_2-R). This is in line with the observations of Camara *et al*. [15], who found no detectable amounts of radical formation on methylene groups next to a tertiary methine group. The lack of reactivity of these CH_2 bonds is probably due to steric hindrance and entropy effects [33].

Table 5.6. Ratio (%) of radicals produced by hydrogen abstraction from n-alkanes by the cumyloxy- radical (n=3)

CH-bond	*n*-hexane	*n*-octane	*n*-decane
CH_3-CH_2-CH_2-	7	<5	<5
CH_3-***CH_2***-CH_2-	54	38	30
CH_3-CH_2-***CH_2***-CH_2-	39	27	20
CH_3-$(CH_2)_2$-***CH_2***-CH_2-	--	32	23
CH_3-$(CH_2)_3$-***CH_2***-CH_2-	--	--	23

Table 5.7. Ratio (%) of radicals produced by hydrogen abstraction from isoalkanes by the cumyloxy- radical (n=3)

CH-bond	2-methylpentane	2-methylhexane
(CH_3)$_2$-CH-CH_2-	14	8
$(CH_3)_2$-***CH***-CH_2-	45	35
$(CH_3)_2$-CH-***CH_2***-CH_2-	17	12
$(CH_3)_2$-CH-CH_2-***CH_2***-CH_3	24	--
$(CH_3)_2$-CH-CH_2-***CH_2***-CH_2-CH_3	--	18
$(CH_3)_2$-CH-$(CH_2)_2$-***CH_2***-CH_3	--	27

To a lower extent, unsaturated reaction products are observed. The presence of these unsaturated alkanes species indicates that after hydrogen abstraction a low number of disproportionations of the alkyl-radicals [2] and a higher number of disproportionations of the alkane dimers radicals take place. The latter result in unsaturated alkane dimers. This indicates a disproportionation reaction of the alkane dimer radicals, rather than of the alkane-substrate radicals. The relative concentrations of the disproportionation products for each alkane are given in

Table 5.8. The relative concentration increases with increasing chain length and the presence of a methine group. Experiments with lower DCP concentration (0.5%, *w/w*) did not significantly affect the relative concentrations of the disproportionation products. No indication of a scission reaction was found, which is probably related to negligible steric effects in these low-molecular-weight model compounds [34, 35].

The current results for a series of low-molecular-weight alkanes, both linear and branched, should be used with care when translating them to the EP(D)M-polymer system. The results indicate that the combination reaction of branched alkanes (*e.g.* EPM) occurs preferably on the tertiary methine groups and to a lower extent on the secondary methylene groups, especially when the methylene group is located next to a methine group. On the other hand, it is confirmed that hydrogen abstraction from branched hydrocarbons does not proceed with extreme selectivity, since primary methyl groups are also involved in hydrogen abstraction. The result will be a distribution of combination sites along the polymer chain, which is in agreement with some theoretical calculations [36]. The results indicate that the reactivity is not only controlled by enthalpy effects, but also by entropy and steric effects. This was also suggested by Sylvain [37], who found that steric effects control the reactivity of hindered radicals, while the reactivity of small unhindered radicals is controlled by enthalpy effects.

Table 5.8. Relative concentration (%) of disproportionation products on total concentration dimers formed from n-alkanes and isoalkanes with DCP (n=3)

Substrate	**%** disproportionation products
n-hexane	2.1
n-octane	3.0
n-decane	6.3
2-methylpentane	6.6
2-methylhexane	11.1

5.4. Conclusion

The reaction products of a series of linear and branched alkanes heated in the presence of DCP have been separated by both GC, using a non-polar column, and GC×GC. In both cases, the compounds were detected by MS. The different isomeric reaction products were identified using an optimised ionisation energy of 55 eV and careful assignment of the high-mass *m*/*z* ions. To increase the

reliability of the elucidated structures, a QSPR model was used to predict the boiling points and, subsequently, the GC retention times and the elution order. This indirect QSPR approach is feasible for these kinds of compounds, especially for alkanes with a low degree of branching. However, long-chain branched alkanes (propyl and butyl-side chains) show an increasing deviation between experimental retention times and those calculated by the indirect QSPR model. Using a direct relation between structural parameters and GC retention times the deviations for highly branched C16 and C20 alkanes was significantly improved. Less improvement was observed for the shorter-chain (C12 and C14) branched alkanes. In spite of these systematic deviations, the elution order of all the reaction products could be predicted well, confirming the structures derived from MS-fragmentation patterns and from the GC×GC chromatograms.

Quantification of the different identified products with GC-FID showed that a significant fraction of the reaction products undergoes a disproportionation reaction. The selectivity of hydrogen abstraction from the alkanes roughly follows the statistical distribution of the various methylene groups. The hydrogen abstraction from a methylene group next to a primary methyl group (CH_3-$\boldsymbol{CH_2}$-CH_2-R) was found to occur more frequently than expected from the statistical distribution of the methylene groups, while the hydrogen abstraction from methylene groups next to an ethyl group (CH_3-CH_2-$\boldsymbol{CH_2}$-CH_2-R) occurred systematically less often. The same holds for isoalkanes, which showed a lower probability of hydrogen abstraction from the methylene group next to an ethyl group ((CH_3)$_2$-CH-CH_2-$\boldsymbol{CH_2}$-CH_2-CH_3).

In this study low-molecular-weight (methyl-)alkane model compounds were used to mimic the peroxide combination cross-linking of EP(D)M. A consistent set of results was obtained, which enhances our understanding of the mechanism of peroxide cross-linking of (branched) alkanes. In turn, this can be used to obtain more insight into structure–properties relationships of EP(D)M. The approach used and the results observed form the starting point for a subsequent study into the addition reactions between alkyl-radicals and alkenes (addition cross-linking reaction).

References

[1] J.A. Brydson, Rubbery Materials and their Compounds, Elsevier, London, 1988.

[2] W. Hofmann, Kautsch. Gummi Kunstst. 40 (1987) 308.

[3] F.C.-Y. Wang, D.J. Lohse, B.R. Chapman, B.A. Harrington, J.

Chromatogr. A 1138 (2007) 225.
[4] H.G. Dikland, Kautsch. Gummi Kunstst. 49 (1996) 413.
[5] K. Fujimoto, K.Wataya, J. Appl. Polym. Sci. 13 (1969) 2513.
[6] V.M. Litvinov,W. Barendswaard, M. van Duin, Rubber Chem. Technol. 71 (1998) 105.
[7] V.M. Litvinov, M. van Duin, Kautsch. Gummi Kunstst. 55 (2002) 460.
[8] V.M. Livinov, Macromolecules 39 (2006) 8727.
[9] R. Winters,W. Heinen, M.A.L. Verbruggen, J. Lugtenburg, M. van Duin, H.J.M. de Groot, Macromolecules 35 (2002) 1958.
[10] R. Peters, J. van der Weerd, V. Litvinov, M. van Duin, in preparation.
[11] C.G. Moore, L. Mullins, P.Mc.L. Swift, J. Appl. Polym. Sci. 5 (1961) 293.
[12] F.K. Lautenschleager, K. Edwards, Rubber Chem. Technol. 53 (1979) 213.
[13] H.M. van den Berg, J.W. Beulen, E.F.J. Duynstee, H.L. Nelissen, Rubber Chem. Technol. 57 (1984) 265.
[14] J.D. van Drumpt, H.H.J. Oosterwijk, J. Polym. Sci. 14 (1976) 1495.
[15] S. Camara, B.C. Gilbert, R.J. Meier, M. van Duin, A.C. Whitwhood, Org. Biomol. Chem. 1 (2003) 1181.
[16] M. van Duin, H.G. Dikland, Rubber Chem. Technol. 76 (2003) 132.
[17] H. Dikland, M. van Duin, in: V.M. Litvinov, P.P. De (Eds.), Spectroscopy of Rubber and Rubbery Materials, Rapra Technology, Shawbury, 2002 (Chapter 6).
[18] R.L. Grob, E.F. Barry, Modern Practice of Gas Chromatography, 4th ed., Wiley-Interscience, New York, 2004.
[19] F.W. Mc-Lafferty, Interpretation of Mass Spectra, 3rd ed., University Science Books, Mill Valley, CA, 1980.
[20] J.B. Phillips, J. Beens, J. Chromatogr. A 856 (1999) 331.
[21] F.T. Eggertson, S. Groennings, J.J. Holst, Anal. Chem. 32 (1960) 904.
[22] Data from Database Crossfire Beilstein (Online), Beilstein Institut zur Förderung der Chemischen Wissenschaften, Frankfurt amMain, DE, April 2007, http://www.beilstein.com/products/xfire.
[23] Data from the US National Institute of Standards and Technology (NIST), NIST Standard Reference Database 69, NIST ChemistryWebBook, June 2005 Release, http://webbook.nist.gov/ chemistry.
[24] T.M.Westerbrug, K.J. Dawson, K.W. McLaughlin, Endeavor 1 (2005) 1.
[25] A.R. Katritzky, K. Chen, U. Maran, D.A. Carlson, Anal. Chem. 72 (2000) 101.
[26] V.E.F. Heinzen, M.F. Soared, R.A. Yunes, J. Chromatogr. A 849 (1999) 495.
[27] N. Dimov, A. Osman, Anal. Chim. Acta 323 (1996) 15.
[28] O. Mekenyan, N. Dimov, V. Enchev, Anal. Chim. Acta 260 (1992) 69.
[29] K.J. Burch, D.K. Wakefield, E.G. Whitehead, MATCH-Commun.

Math. Comput. Chem. 47 (2003) 25.
[30] H. Hosoya, Bull. Chem. Soc. Jpn. 44 (1971) 2332.
[31] J. Lal, J.E. McGrath, R.D. Board, J. Polym. Sci. 6 (1968) 821.
[32] L.D. Loan, J. Polym. Sci. 2 (1964) 3053.
[33] S. Camara, B.C. Gilbert, R.J. Meier, M. van Duin, A.C. Whitwood, Polymer 47 (2006) 4683.
[34] P. Sajkiewicz, P.J. Phillips, J. Polym. Sci. 33 (1995) 853.
[35] G.N. Patel, A. Keller, J. Polym. Sci. 11 (1973) 737.
[36] M. van Duin, B. Coussens, Presented at Polymer Processing Society, vol. 11, Stuttgart, 1995.
[37] M. Sylvain, Presented at Extrusion Reactive, Lyon-Villeurbanne, 2007.